











Original Research Article

Molecular Docking and ADMET-Based Discovery of *Glycyrrhiza glabra* Bioactives as P-Glycoprotein Inhibitors for Combating Multidrug Resistance

Karthickeyan Krishnan¹, S. Gopi Krishnan², Ch K V L S N Anjana Male^{3,*}, Pericharla Venkata Narasimha Raju⁴, Phanindra Erukulla⁵, Kanaka Durga Hanumanthu⁶, Ashutosh Pathak⁷, Nampelly Karnakar^{8,*}

¹Department of Pharmacy Practice, School of Pharmaceutical Sciences, Vels Institute of Science, Technology and Advanced Studies (VISTAS), Pallavaram, Chennai 600 117, India

²Department of Pharmacology, Arulmigu Kalasalingam College of Pharmacy, Krishnankoil, Viridhunagar Dist., Tamil Nadu, India

³School of Pharmacy, ITM University, Gwalior, Madhya Pradesh, India

⁴Department of Regulatory Affairs, Hikma Pharmaceuticals USA Inc., 2 Esterbrook Lane, Cherry Hill, NJ 08003, USA

⁵Department of Regulatory Affairs, Ricon Pharma LLC, 100 Ford Rd, Suite #9, Denville, NJ 07834, USA

⁶KL Business School, Koneru Lakshmaiah Education Foundation, Vaddeswaram, Guntur, Andhra Pradesh 522502, India

⁷Department of Pharmacy Practice, Teerthanker Mahaveer College of Pharmacy, Teerthanker, Mahaveer University, Moradabad, UP 244001, India

⁸Department of Pharmaceutics, Malla Reddy Institute of Pharmaceutical Sciences, Malla Reddy Vishwavidyapeeth (Deemed to be University), Secunderabad, 500100, Telangana, India

ARTICLE INFO

Article history

Submitted: 2025-10-06

Revised: 2025-11-08

Accepted: 2025-11-16

ID: AJCA-2510-1952

DOI: [10.48309/ajca.2026.553659.1952](https://doi.org/10.48309/ajca.2026.553659.1952)

KEYWORDS

Glycyrrhiza glabra

P-glycoprotein

Multidrug resistance

Molecular docking

ADMET analyses

Natural P-gp inhibitors

ABSTRACT

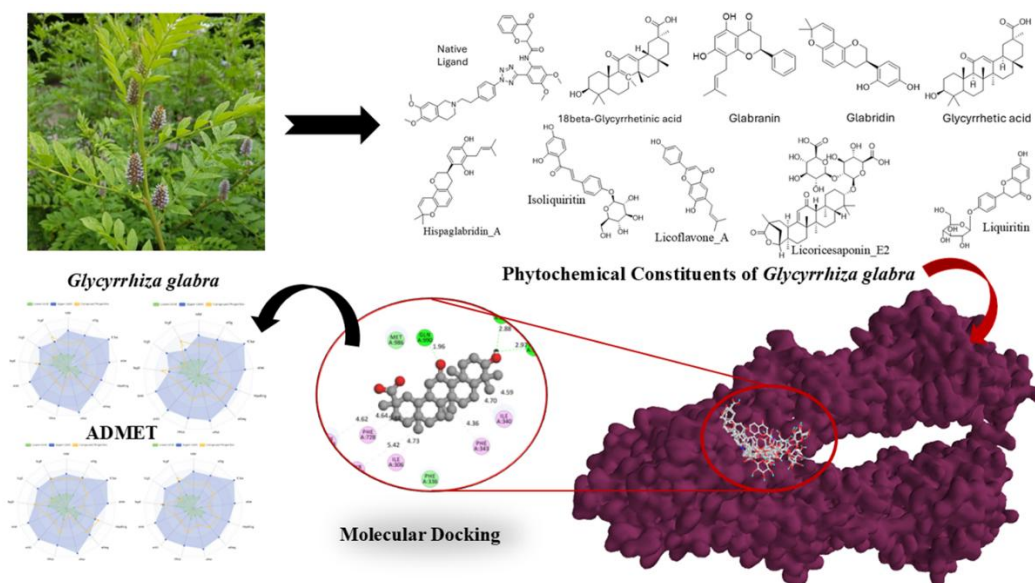
This study employed an extensive computational approach to identify bioactive compounds from *Glycyrrhiza glabra* (licorice) with potential inhibitory activity against P-glycoprotein (P-gp), a key efflux transporter associated with multidrug resistance (MDR) in cancer. Twenty phytochemicals, including triterpenoid saponins, flavonoids, and chalcones, were evaluated using molecular docking and *in silico* ADMET analyses. Docking studies using AutoDock Vina against the human P-gp structure (PDB ID: 7O9W) revealed several compounds exhibiting stronger binding affinities than the standard inhibitor verapamil (−7.8 kcal/mol). Among them, 18β-glycyrrhetic acid (−9.7 kcal/mol), glabridin (−9.3 kcal/mol), glabranin (−9.1 kcal/mol), and licoflavone A (−8.7 kcal/mol) showed the most stable interactions with key residues PHE343, GLN347, GLU875, and TYR310, crucial for substrate recognition and transport inhibition. ADMET analyses indicated that glabridin, glabranin, and licoflavone A possess high gastrointestinal absorption, non-hepatotoxicity, and favorable oral bioavailability, satisfying Lipinski and Veber's drug-likeness criteria. Conversely, glycosylated saponins displayed lower permeability, but minimal toxicity, suggesting potential combinatorial benefits. Overall, glabridin, glabranin, and licoflavone A have emerged as promising natural P-gp inhibitors capable of reversing MDR in cancer, meriting further *in vitro* and *in vivo* validation.

* Corresponding author: Anjana Male, Ch K V L S N/ Karnakar, Nampelly

✉ E-mail: anjana.male@gmail.com / karnakar.nampelly@mrvv.edu.in

© 2026 by SPC (Sami Publishing Company)

GRAPHICAL ABSTRACT



Introduction

Multidrug resistance (MDR) remains one of the most significant obstacles to successful cancer treatment, often leading to therapeutic failure and disease recurrence [1–3]. Overexpression of P-glycoprotein (P-gp), a 170 kDa ATP-binding cassette (ABC) transporter produced by the ABCB1 gene, is a major cause of MDR. P-gp actively transports a variety of chemotherapeutic agents, including doxorubicin, paclitaxel, and vincristine, out of cancer cells. This process decreases intracellular concentrations and reduces therapeutic efficiency [4,5]. This transporter-mediated efflux not only leads to resistance to medications with different structures and functions, but also makes therapy less effective, which is a major problem in cancer care. Consequently, the identification of effective and safe P-gp inhibitors is a viable approach to counteract MDR and re-establish drug sensitivity in cancer treatment [4–7].

In the last several decades, many generations of synthetic P-gp inhibitors such as verapamil, cyclosporine A, and tariquidar have been

produced and tested. Most of them have failed in human trials; however, because they have undesirable side effects, they inhibit too many targets at once, and interact with other medications in ways that render them less effective [8–10]. Consequently, emphasis has shifted toward identifying natural P-gp inhibitors derived from medicinal plants. These compounds often exhibit multitarget efficacy, reduced toxicity, and improved biocompatibility. *Glycyrrhiza glabra* L. (licorice), a perennial plant belonging to the Fabaceae family, has garnered significant interest because of its abundant phytochemical variety and wide pharmacological attributes [11,12].

Glycyrrhiza glabra has been extensively used in traditional medicinal systems, including Ayurveda, Traditional Chinese Medicine (TCM), and Unani, for its anti-inflammatory, antibacterial, hepatoprotective, and anticancer properties. Phytochemical analyses of licorice roots have revealed a complex mixture of triterpenoid saponins, flavonoids, isoflavones, chalcones, and coumarins, many of which exhibit significant biological activities relevant to cancer prevention

and therapy [13,14]. Key constituents, such as glycyrrhizin, glabridin, licochalcone A, liquiritigenin, isoliquiritigenin, and 18 β -glycyrrhetic acid have demonstrated antioxidant, anti-inflammatory, apoptotic, and anti-proliferative effects in various cancer models [13–16]. Importantly, several flavonoid and triterpenoid compounds from licorice have been reported to modulate efflux transporters, including P-gp, by interacting with their transmembrane domains or by altering their expression. This indicates their strong potential as natural modulators of MDR [17].

Recent advances in computational biology and cheminformatics have revolutionized the process of drug discovery by enabling *in silico* screening of large compound libraries to identify potential bioactive molecules with high affinity for target proteins. Molecular docking, molecular dynamics (MD) simulations, and Absorption, Distribution, Metabolism, Excretion, and Toxicity (ADMET) prediction tools provide powerful platforms to explore ligand–target interactions at the atomic level, predict pharmacokinetic behavior, and filter compounds based on drug-likeness criteria. Such computational approaches significantly reduce experimental costs and time, while increasing the probability of identifying promising lead candidates [18–21].

This study used a computational approach to identify possible P-gp inhibitors from bioactive chemicals extracted from *Glycyrrhiza glabra*. Twenty structurally varied chemicals, including triterpenoids, flavonoids, and saponins, were chosen based on a comprehensive literature review and existing pharmacological data. The molecular docking and ADMET studies were used to test these compounds and determine whether they would bind to P-gp inhibitors and how they would interact with them. The binding interactions were examined to identify critical amino acid residues that contribute to ligand stability inside the P-gp binding pocket, while

ADMET profiling evaluated their safety, bioavailability, and drug-like properties.

This study was based on the concept that bioactive chemicals derived from licorice may decrease P-gp activity, consequently augmenting intracellular drug retention and reversing MDR in cancer cells. Finding these molecules could result in a natural and safer alternative to synthetic inhibitors, which would help develop further treatments that increase the effectiveness of chemotherapy. This study connects traditional medicine and molecular pharmacology by combining ethnopharmacological expertise with current computational techniques. This provides useful information on how to create new P-gp modulators from *Glycyrrhiza glabra* to combat MDR in cancer.

Experimental

Selection of compounds

A comprehensive literature review was performed to ascertain the bioactive components of *Glycyrrhiza glabra* (licorice) that have notable pharmacological potential. The main sources were two in-depth studies: Dang *et al.* in Acupuncture and Herbal Medicine and Pastorino *et al.* in Phytotherapy Research. Together, these reviews included more than 300 different phytoconstituents of licorice roots and rhizomes [13,22]. These compounds are mostly triterpenoid saponins, flavonoids, and phenolic compounds. They are known for their anti-inflammatory, antioxidant, liver-protective, and antibacterial effects.

Based on these reports, twenty representative compounds were selected for computational, structural, and pharmacokinetic screening in the present study (Figure 1). The selection criteria included structural diversity, strong and stable molecular frameworks (flavonoid or triterpenoid skeletons), reported bioactivity in experimental studies, and availability of validated molecular data in public databases, such as PubChem.

Molecular docking analysis

A molecular docking study was performed to predict the binding affinity and interaction of bioactive compounds from *Glycyrrhiza glabra* with P-gp, with the aim of identifying potential inhibitors for overcoming MDR [18–21].

Preparation of ligands

The chemical structures of 20 selected bioactive compounds were determined using ChemDraw and converted into three-dimensional (3D) conformers. Structures were retrieved or confirmed from the PubChem database, and energy minimization was performed to obtain stable conformations suitable for docking studies.

Preparation of target protein

The crystal structure of P-gp (PDB ID: 709W) was obtained from the RCSB Protein Data Bank (PDB). Proteins were prepared by removing water molecules, heteroatoms, and co-crystallized ligands using Discovery Studio. Polar hydrogens were added and the protein structure was optimized for docking.

Docking protocol

Molecular docking was performed using PyRx, which employs the AutoDock Vina algorithm for flexible ligand docking. The binding site coordinates were defined as X: 150.925275, Y: 141.413252, and Z: 164.206523. A grid box was centered on these coordinates to ensure that the ligands comprehensively explored the active sites. Docking simulations were performed using default exhaustiveness and the best binding poses were selected based on the binding energy (kcal/mol) and interaction profiles.

Analysis of docked complexes

The docked complexes were visualized and analyzed using Discovery Studio to evaluate hydrogen bonding, hydrophobic interactions, π - π stacking, and other non-covalent interactions. Binding affinity and interaction residues were documented for comparison among all ligands [18–21]. A 3D view of the P-gp with an active cavity is shown in Figure 2.

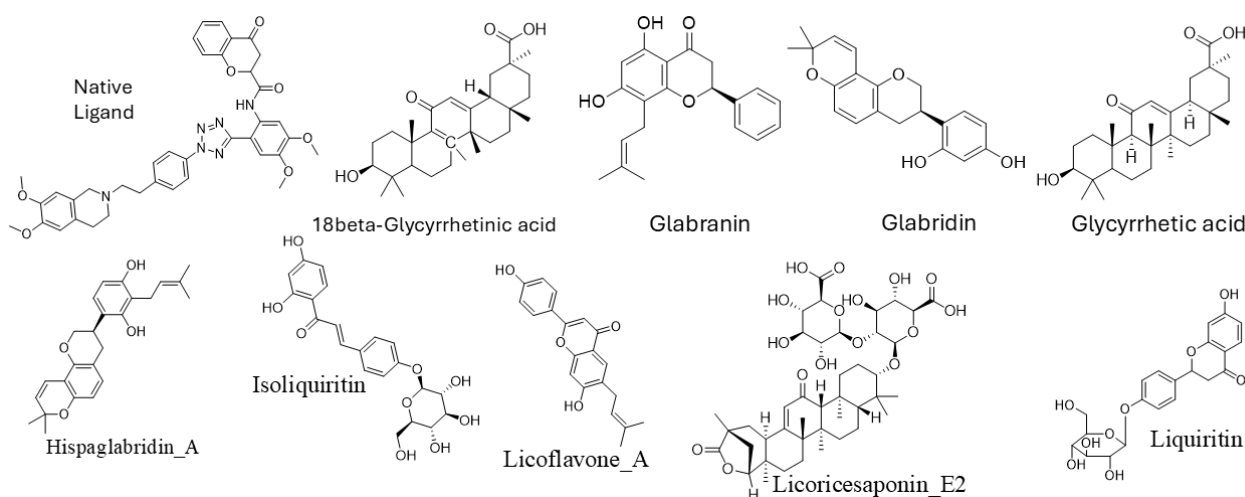


Figure 1. Chemical structures of the most potent compounds. The figure illustrates the structural diversity of key phytoconstituents, including triterpenoids and flavonoids, which demonstrated high binding affinities in docking analyses.

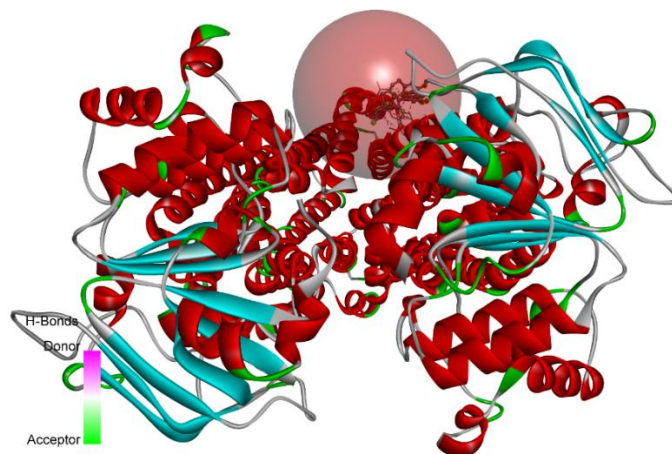


Figure 2. 3D representation of the P-gp active cavity complexed with the native ligand. The figure highlights the binding pocket architecture and key residues involved in ligand recognition and stabilization within the transmembrane domain of P-gp.

In silico ADMET analyses

To assess the pharmacokinetic and safety profiles of the selected compounds, *in silico* ADMET analysis was conducted using the optimized 3D structures obtained from ChemDraw and PubChem, with ligand formats modified to provide connectivity with web-based solutions. The ADMET properties were predicted using SwissADME and ADMETlab 3.0, encompassing absorption parameters such as Caco-2 and MDCK permeability, P-gp substrate/inhibitor potential, and human intestinal absorption (HIA); distribution metrics including plasma protein binding (PPB), volume of distribution (VD), blood–brain barrier (BBB) permeability, and fraction unbound (Fu); metabolism profiling via cytochrome P450 (CYP) enzyme inhibition and substrate specificity (CYP1A2, CYP2C9, CYP2C19, CYP2D6, and CYP3A4); excretion parameters including clearance (CL) and half-life ($T_{1/2}$); and toxicity endpoints such as Ames mutagenicity, hepatotoxicity, drug-induced liver injury (DILI), rat oral acute toxicity, FDA maximum recommended daily dose (FDAMDD), skin sensitization, carcinogenicity, eye corrosion/irritation, and respiratory toxicity.

Furthermore, environmental toxicity was evaluated using the bioconcentration factor (BCF), IG_{50} , and lethal concentrations (LC_{50}) for fish and *Daphnia*. The compiled ADMET parameters enabled a comparative assessment to identify the most promising compounds with optimal pharmacokinetic profiles and minimal toxicity risk [18–21].

Results and Discussion

Molecular docking analysis

A molecular docking investigation of bioactive compounds from *Glycyrrhiza glabra* was conducted to determine whether they could inhibit P-gp, which is a critical efflux transporter linked to MDR in cancer and microbial infections. The findings demonstrated different binding affinities, interaction types, and energy profiles, suggesting that many phytoconstituents of *G. glabra* have significant potential to regulate P-gp activity. The ligands that scored the best in the docking tests were 18 β -glycyrrhetic acid, glycyrrhetic acid, hispaglabridin A, licorice saponin E2, glabridin, and liquiritin. This indicated that they had high binding affinities and were stable in the active site of P-gp. The binding interactions of the selected compounds with P-gp

are illustrated in Table 1. The 2D and 3D binding interactions of the most potent compounds with P-gp are shown in Table 2.

Comparative binding affinity

The docking scores ranged from -6.8 to -9.7 kcal/mol, indicating that the interactions with the target protein were moderate to strong. The native ligand had a docking score of -7.8 kcal/mol, which was used as a point of reference for comparison. 18 β -glycyrrhetic acid and glycyrrhetic acid both had the highest docking scores of -9.7 kcal/mol, which were better than the native ligand and showed that they possess a stronger binding affinity. Hispaglabridin A (-9.3 kcal/mol), licoricesaponin E2 (-8.5 kcal/mol), glabridin (-8.3 kcal/mol), and licoflavone A (-8.4 kcal/mol) also exhibited good binding interactions, suggesting that they might be significant P-gp inhibitors. Other drugs, including glabranin (-8.4 kcal/mol), isoliquiritin (-8.1 kcal/mol), and liquiritin (-8.7 kcal/mol), had slightly lower but significant affinities, indicating potential synergistic or supportive roles in P-gp inhibition.

Nature of interactions and active site residues

A study of hydrogen bonding and hydrophobic interactions showed that the ligands fit into important binding sites of P-gp and create stable connections with residues that are essential for recognizing and moving substrates. Hydrogen bonds, carbon-hydrogen bonds, π - π stacking, and alkyl or π -alkyl hydrophobic interactions among molecules. GLN347, GLU875, GLN990, ILE340, PHE343, PHE728, TYR307, LEU339, and VAL345 are the amino acids that frequently appear as interacting residues. This demonstrates the significance of maintaining stable ligand-protein complexes.

18 β -Glycyrrhetic acid forms many hydrogen bonds with GLN347, GLU875, and GLN990, as well as hydrophobic interactions with ILE340, ILE306,

and PHE343. This large network of interactions explains why it has a high binding score (-9.7 kcal/mol) and implies that it might be a powerful inhibitor. Glycyrrhetic acid also forms hydrogen bonds with PHE728 and hydrophobic interactions with residues such as ILE306, TYR310, TRP232, and PHE343. This resulted in a similar docking score of -9.7 kcal/mol. The existence of π -alkyl and π -sigma contacts increases its stability in the hydrophobic cavity of P-gp, which may block efflux channels.

Hispaglabridin A contacts both the hydrogen and hydrophobic molecules. For example, it forms a carbon-hydrogen bond with ILE340 and alkyl or π -alkyl bonds with LEU339, ILE306, and TYR310. These residues are part of the hydrophobic core of P-gp, which means that the molecule can prevent changes in shape that are needed for drug transport. Hispaglabridin A has a docking score of -9.3 kcal/mol and a ligand energy of 1089.34 kcal/mol, which means that it binds strongly and is in the best position in the active pocket.

Glabridin and glabranin also showed multiple stabilizing interactions. Glabridin forms hydrogen bonds with GLN946, along with electrostatic (π -anion) interactions involving GLU875 and several hydrophobic contacts with PHE343, LEU339, and ILE340. These residues overlapped with those of the native ligand, suggesting competitive inhibition at the active site. The docking score of -8.3 kcal/mol and ligand energy of 1042.65 kcal/mol reflect an energetically favorable configuration. Glabranin formed hydrogen bonds with TYR307 and multiple aromatic π - π stacking interactions with PHE728 and PHE343, consistent with its docking score of -8.4 kcal/mol.

Saponins and flavonoids as key inhibitors

Saponins such as licoricesaponin E2, licoricesaponin A3, and uralsaponin C displayed considerable docking scores between -7.2 and -8.5 kcal/mol. Licoricesaponin E2 formed strong hydrogen bonds with VAL345 and GLY346,

hydrophobic interactions with ILE205 and LEU219, and multiple aromatic contacts with PHE200–PHE204. The consistent involvement of phenylalanine residues suggests aromatic stacking stabilization, which may hinder P-gp substrate binding. Licoricesaponin A3 also had carbon-hydrogen bonds with PRO223 and alkyl interactions with VAL345 and PHE200, which indicated that it might moderately inhibit (–7.4 kcal/mol). Uralsaponin C formed several hydrogen bonds (ALA230 and SER349) and hydrophobic interactions with PRO223 and VAL345, which helped to maintain the stability of the complex in the transmembrane region.

Licoflavone A, formononetin, echinatin, and quercetin are flavonoids with good binding characteristics. Licoflavone A had a docking score of –8.4 kcal/mol, and the main interactions were π -sigma and π - π between PHE343, PHE728, and PHE983. The large hydrophobic surface area indicates that the van der Waals forces are strong. Formononetin and echinatin both formed hydrogen bonds with GLN725 and TYR307 and π - π stacking with PHE728 and PHE983. However, their lower scores (–7.2 kcal/mol) show that they bind slightly less strongly than triterpenoids. Quercetin, a recognized P-gp inhibitor, exhibited modest affinity (–7.2 kcal/mol) while underscoring the significance of hydrogen bonding (GLN195, GLN347) and hydrophobic interactions in P-gp inhibitory processes.

Other compounds

The glycosylated flavonoids liquiritin and liquiritin apioside had good docking scores of –8.7 and –6.8 kcal/mol, respectively. Liquiritin formed hydrogen bonds with GLY62 and GLN195 and π - π stacking interactions with PHE343 and ILE306, which made it very stable. Glycosylation probably strengthens hydrogen bonding, but it could weaken the hydrophobic fit weaker, which might

explain the slight change in binding energy. Isoliquiritin and neoliquiritin exhibited hydrogen bonding with GLN195, THR199, and GLN946, yielding modest scores (–8.1 and –7.7 kcal/mol). These compounds may function as supplementary inhibitors to enhance the overall inhibitory characteristics of the *G. glabra* components.

Hydrogen bonding and hydrophobic balance

Hydrogen bonds are crucial for creating ligand-receptor complexes that are more selective and stable, whereas hydrophobic interactions are assisted by binding affinity and pocket fitting. Compounds with more than one regular hydrogen bond, such as 18 β -glycyrrhetic acid, glycyrrhetic acid, hispaglabridin A, and licoricesaponin E2, had better docking scores. In contrast, ligands that had mostly π - π or π -alkyl interactions, such as glabridin and licoflavone A, were similarly very stable because they were stacked with phenylalanine and tyrosine residues. It appears that the interaction between hydrogen bonding and hydrophobicity is important for determining the mechanism of P-gp inhibition.

Overall structure–activity relationship (SAR)

A distinct SAR was identified. Triterpenoids, including glycyrrhetic acid derivatives, exhibit the most significant inhibitory potential due to their rigid hydrophobic structures and carboxylic functions, which facilitate deep penetration into the P-gp binding cavity and the formation of numerous hydrogen bonds. Flavonoids and chalcones, which possess planar aromatic rings, prefer π - π stacking with the aromatic residues. On the other hand, saponins utilize their glycosidic linkages to form additional hydrogen bonds, which stabilize the complex through polar interactions.

Table 1. Binding interactions of selected compounds with P-glycoprotein

Amino acid	Bond length	Bond type	Bond category	Ligand energy (Kcal/mol)	Docking score
native ligand					
VAL345	3.7575		Pi-sigma		
PHE200	4.98263				
PHE200	4.96028				
PHE204	4.99912	Hydrophobic	Alkyl	805.9	-7.8
LEU219	5.17873				
VAL345	4.19977				
PHE204	5.27269		Pi-Alkyl		
18beta-Glycyrrhetic_acid					
GLN347	2.97005				
GLU875	2.8752	Hydrogen bond	Conventional hydrogen bond		
GLN990	1.95681				
ILE340	4.59037				
ILE306	4.73326		Alkyl		
ILE340	4.69688			1067.25	-9.7
TYR310	5.42256				
PHE343	4.36174	Hydrophobic			
PHE728	5.47958		Pi-Alkyl		
PHE728	4.63926				
PHE983	4.62214				
Echinatin					
PHE343	3.96578		Pi-Pi Stacked		
LEU339	5.3441	Hydrophobic		148.86	-7.2
ILE340	5.39449		Pi-Alkyl		
Formononetin					
TYR307	2.3101				
GLN725	1.9232	Hydrogen bond	Conventional hydrogen bond		
PHE728	4.39724			171.09	-7.2
PHE728	4.90158	Hydrophobic	Pi-Pi Stacked		
PHE983	4.03678				
Glabranin					
TYR307	2.44076	Hydrogen bond	Conventional hydrogen Bond		
LEU339	3.57488		Pi-sigma		
PHE728	4.16606		Pi-Pi stacked		
PHE343	5.27651		Pi-Pi T-shaped		
ILE340	5.49796			239.69	-8.4
PHE336 -	5.12659	Hydrophobic			
PHE336	4.64609		Pi-Alkyl		
PHE983	4.99056				
PHE983	4.02605				
Glabridin					
GLN946	2.36313	Hydrogen Bond	Conventional Hydrogen Bond	1042.65	-8.3

GLU875	4.84874	Electrostatic	Pi-Anion		
PHE343	5.42648		Pi-Pi stacked		
LEU339	4.74072				
ILE340	5.45541				
ILE306	3.89299		Alkyl		
LEU339	4.8274	Hydrophobic			
ILE340	5.0938				
LEU65	5.24236				
PHE343	3.95807		Pi-Alkyl		
PHE343	3.75013				
Glycyrrhetic acid					
PHE728	2.7057	Hydrogen Bond	Pi-Donor Hydrogen Bond		
PHE343	3.49514		Pi-Sigma		
ILE306	5.23297				
ILE306	4.43527		Alkyl		
ILE306	4.8463				
TRP232	4.88584				
PHE303	5.25444	Hydrophobic		664.42	-9.7
TYR307	4.23507				
TYR310	4.67667				
TYR310	5.4138		Pi-Alkyl		
PHE343	4.82345				
PHE343	4.49412				
PHE728	4.44697				
Glycyrrhizin					
LEU227	2.9935	Hydrogen Bond	Conventional Hydrogen Bond		
LEU219	5.15831				
LEU219	4.53662				
ILE205	5.14905		Alkyl		
LEU219	5.25929				
LEU219	5.33085				
PHE200	5.17942	Hydrophobic		891.68	-7.6
PHE200	4.16797				
PHE201	5.38802				
PHE201	4.58899		Pi-Alkyl		
PHE201	4.71709				
PHE204	3.87634				
PHE204	4.53581				
Hispaglabridin_A					
ILE340	3.57859	Hydrogen Bond	Carbon Hydrogen Bond		
ILE340	3.89044				
ILE306	4.59713				
LEU339	4.88462	Hydrophobic	Alkyl	1089.34	-9.3
MET192	4.26368				
MET192	4.33223				

LEU339 4.94957
 ILE340 4.4266
 LEU65 4.97455
 TYR310 5.13396
 PHE343 4.77141

Pi-Alkyl

Isoliquiritigenin

GLN725	2.13589	Hydrogen bond	Conventional hydrogen bond		
PHE983	4.05122	Hydrophobic	Pi-Pi Stacked	131.2	-6.8
TYR307	5.27482				

Isoliquiritin

THR199	2.46678	Hydrogen bond	Conventional hydrogen bond		
MET192	2.4644				
GLN347	2.34544				
GLN195	2.081	Hydrophobic	Pi-Pi T-shaped	207.92	-8.1
PHE343	5.31813				
ILE340	5.33881				
ILE306	4.91344				
LEU339	5.07707		Pi-Alkyl		

Licochalcone_A

GLN725	3.06739	Hydrogen bond	Conventional hydrogen bond			
TYR307	3.63449		Carbon hydrogen bond			
PHE336	5.63462	Hydrophobic	Pi-Pi Stacked			
PHE983	3.7195					
PHE732	5.57773			Pi-Pi T-shaped		
LEU339	4.64015				283.51	-7.4
ILE306	3.84647			Alkyl		
LEU339	4.28891					
ILE306	5.42616					
PHE343	4.22358		Pi-Alkyl			
PHE343	4.11262					

Licoflavone_A

ILE340	3.88968	Hydrophobic	Pi-Sigma			
PHE343	5.40975		Pi-Pi T-shaped			
ILE340	5.43246					
ILE340	4.92498					
PHE336	4.71666					
PHE728	4.71077				191.99	-8.4
PHE732	4.52703			Pi-Alkyl		
PHE732	4.43134					
PHE983	4.53193					
PHE983	4.35188					

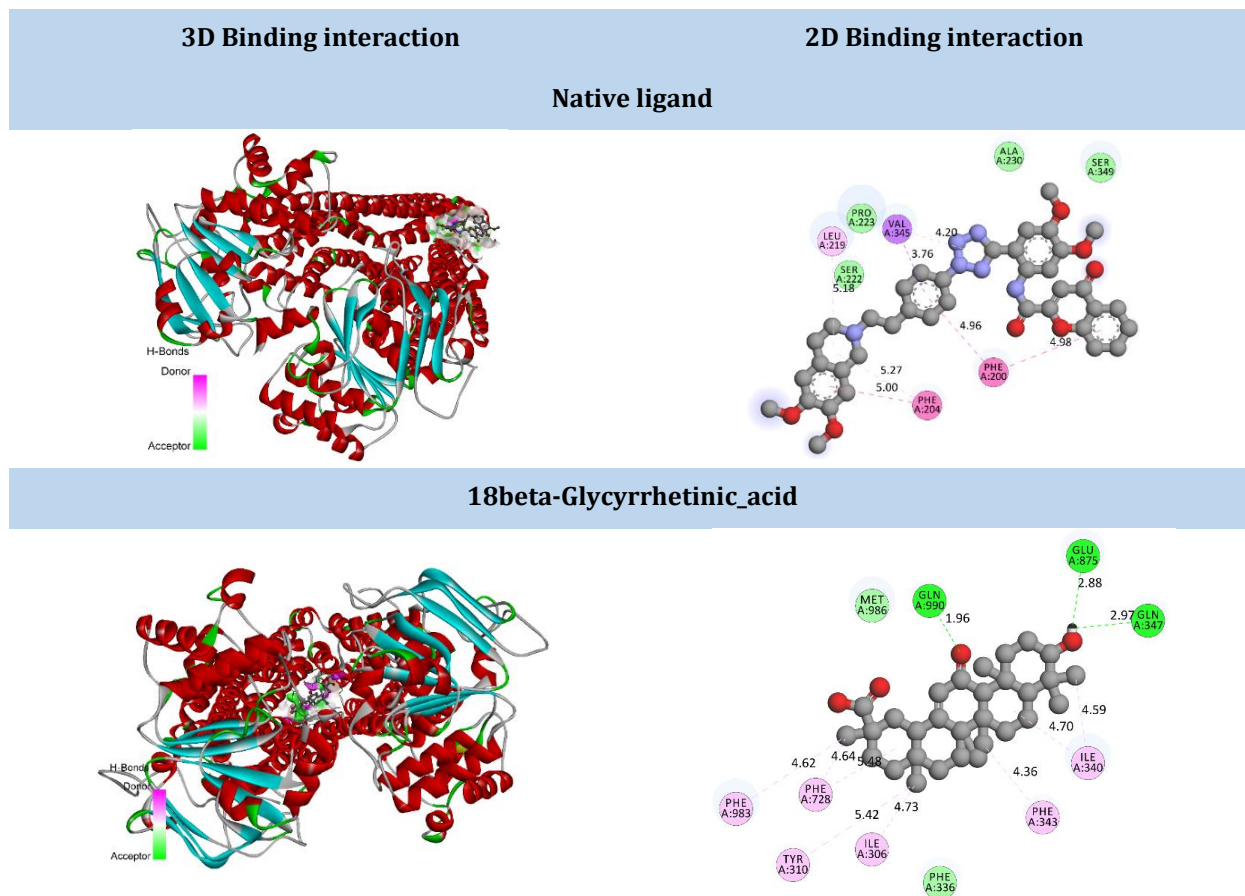
Licoricesaponin_A3

PRO223	3.51282	Hydrogen bond	Carbon hydrogen bond		
VAL345	4.39831	Hydrophobic	Alkyl	904.43	-7.4
PRO223	4.24968				

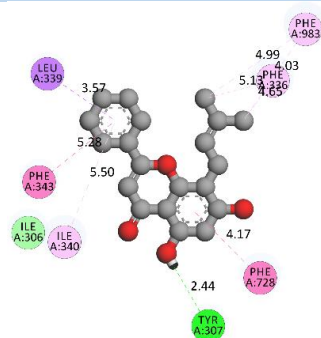
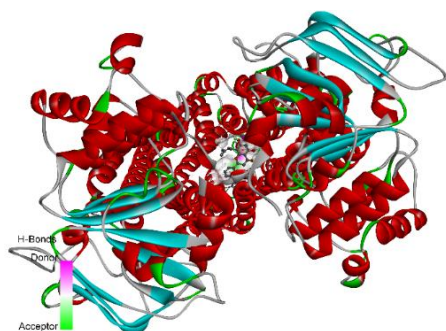
PRO223	4.83737				
LEU227	4.5327				
ALA230	3.86067				
ALA230	4.57888				
VAL345	5.33783				
PHE200	5.10421		Pi-Alkyl		
Licoricesaponin_E2					
VAL345	2.15927		Conventional hydrogen bond		
GLY346	2.33656	Hydrogen bond			
SER349	3.39424		Carbon hydrogen bond		
ILE205	5.0238				
LEU219	5.32033		Alkyl		
PHE200	4.87878				
PHE200	5.43405				
PHE200	5.25755			926.58	-8.5
PHE200	4.06926	Hydrophobic			
PHE201	5.21129		Pi-Alkyl		
PHE201	4.9602				
PHE201	4.79813				
PHE204	5.08286				
PHE204	4.73781				
PHE204	4.45464				
Liquiritigenin					
TYR307	2.35454	Hydrogen bond	Conventional hydrogen bond		
PHE728	3.86399	Hydrophobic	Pi-Pi Stacked	187.4	-6.9
PHE336	4.83784		Pi-Pi T-shaped		
Liquiritin					
GLY62	2.65397	Hydrogen bond	Conventional hydrogen bond		
GLN195	2.65798				
PHE343	3.93696	Hydrophobic	Pi-Pi Stacked	343.25	-8.7
ILE306	4.9064		Pi-Alkyl		
Liquiritin_apioside					
SER349	2.65446	Hydrogen bond	Conventional hydrogen bond		
SER222	2.4472				
PRO223	4.48484		Amide-Pi stacked	399.35	-6.8
VAL345	5.33272	Hydrophobic			
LEU219	5.40866		Pi-alkyl		
PRO223	4.02943				
Neoliquiritin					
GLN946	2.65167				
HIS61	3.0717				
THR199	2.56816	Hydrogen bond	Conventional hydrogen bond	283.23	-7.7
GLN195	2.30349				
GLN946	2.84488				
GLN946	1.90553				

LEU65	3.84945	Hydrophobic	Pi-Sigma		
LEU339	5.02232	Hydrophobic	Pi-Alkyl		
Quercetin					
GLN347	3.07894		Conventional hydrogen bond		
GLN195	2.12366	Hydrogen Bond		181.13	-7.2
ALA348	3.0252		Carbon hydrogen bond		
MET192	4.40456	Hydrophobic	Pi-Alkyl		
Uralsaponin_C					
ALA230	2.96999		Conventional hydrogen bond		
SER349	2.13287	Hydrogen Bond			
SER349	3.60731		Carbon hydrogen bond		
PRO223	3.99531				
VAL345	4.68947				
ILE352	5.19733			886.93	-7.2
ALA230	3.7197		Alkyl		
PRO223	3.45466	Hydrophobic			
ALA230	4.21804				
VAL345	5.23148				
VAL345	4.95273				
PHE200	4.73899		Pi-Alkyl		

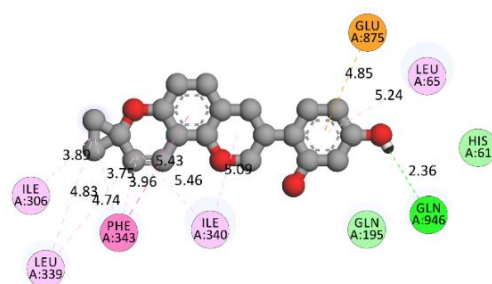
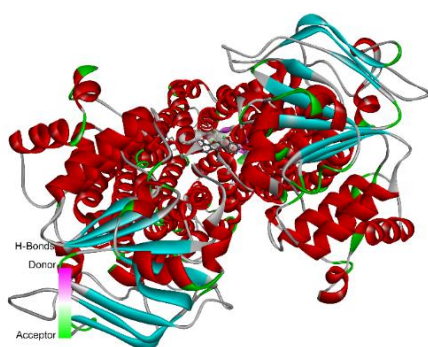
Table 2. 2D and 3D binding interactions of the most potent compounds with P-gp



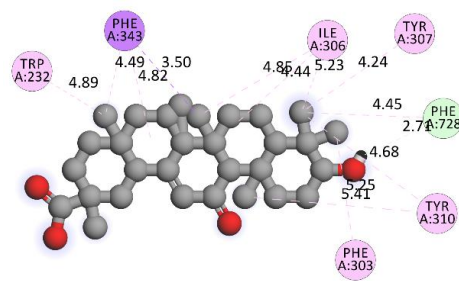
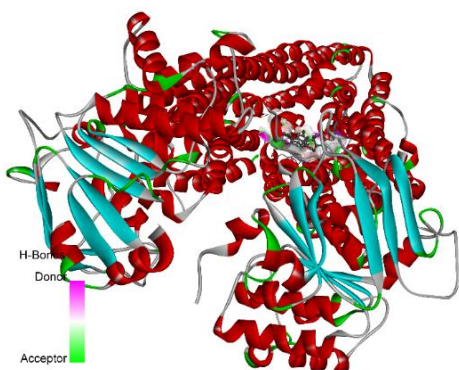
Glabranin



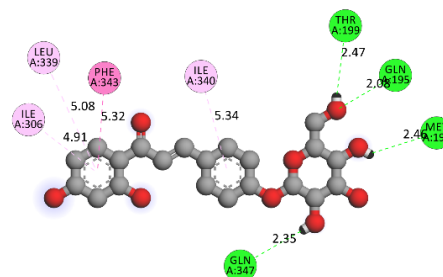
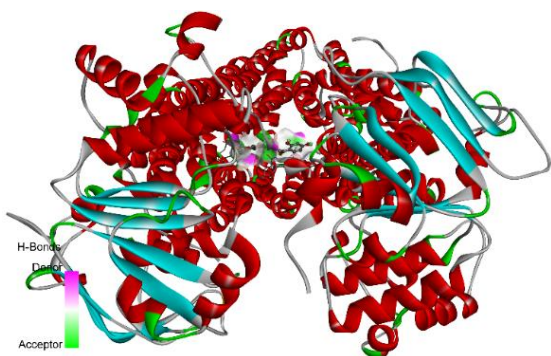
Glabridin



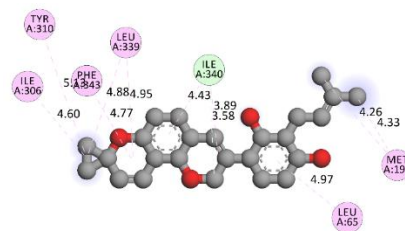
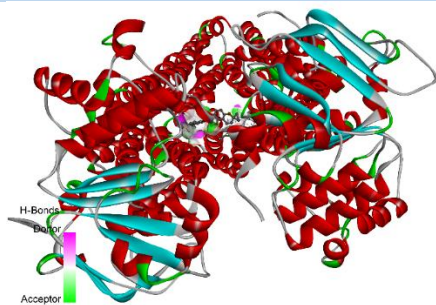
Glycyrrhetic acid



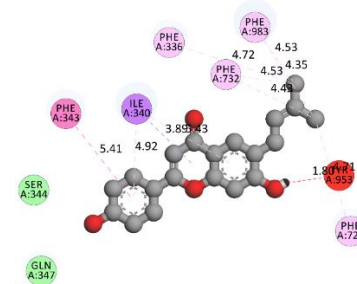
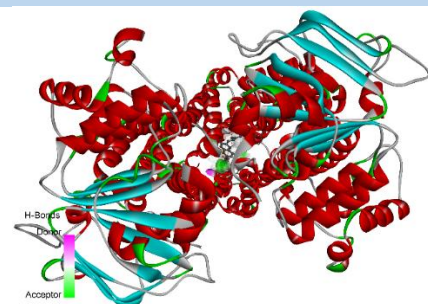
Isoliquiritin



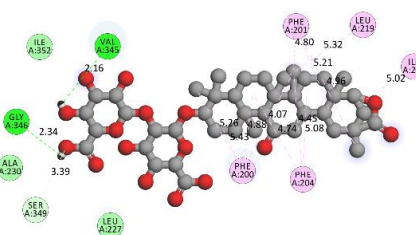
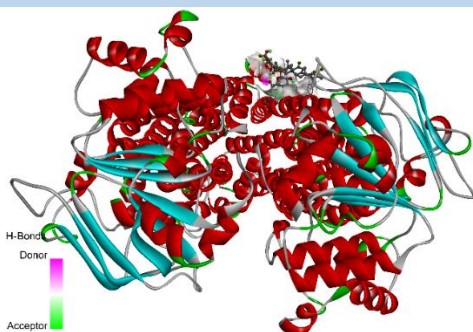
Hispaglabridin_A



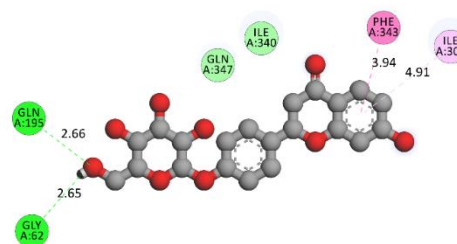
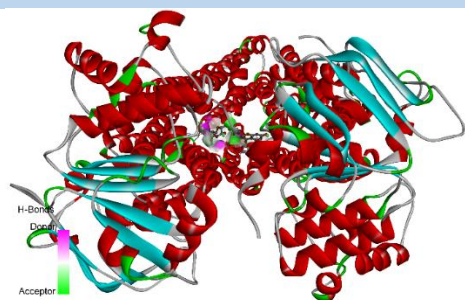
Licoflavone_A



Licoricesaponin_E2



Liquiritin



In silico ADMET analyses

As per the molecular docking analysis, the nine most potent compounds derived from *Glycyrrhiza glabra* and the native ligand were further

evaluated through extensive *in silico* ADMET analysis to assess their pharmacokinetic and safety profiles. These compounds included 18 β -glycyrrhetic acid, glabranin, glabridin, glycyrrhetic acid, hispaglabridin A, isoliquiritin,

licoflavone A, licoricesaponin E2, and liquiritin. The results summarized in Tables 3–8 highlight the physicochemical, drug-likeness, pharmacokinetic, and environmental characteristics that determine their potential as P-gp inhibitors to combat MDR.

Table 3. Physicochemical properties of selected derivatives

Compounds	MW	Volume	Dense	nHA	nHD	nRot	nRing	TPSA	Log S	log P
Native Ligand	690.28	691.2375	0.998615	13	1	12	7	139.16	-5.37799	3.728485
18beta-Glycyrrhetic_acid	470.34	511.9053	0.918803	4	2	1	5	74.6	-4.70727	3.068492
Glabranin	324.14	342.876	0.945356	4	2	3	3	66.76	-5.03051	4.514872
Glabridin	324.14	336.956	0.961965	4	2	1	4	58.92	-4.68808	4.14236
Glycyrrhetic_acid	470.34	511.9053	0.918803	4	2	1	5	74.6	-4.86756	3.111419
Hispaglabridin_A	392.2	420.7995	0.932035	4	2	3	4	58.92	-5.26604	5.483441
Isoliquiritin	418.13	404.1231	1.03466	9	6	6	3	156.91	-3.0227	1.029564
Licoflavone_A	322.12	340.2396	0.946745	4	2	3	3	70.67	-4.77396	3.752484
Licoricesaponin_E2	820.39	793.9975	1.03324	16	7	6	8	256.04	-3.96234	1.314672
Liquiritin	418.13	398.2031	1.050042	9	5	4	4	145.91	-2.75384	0.134691

Table 4. Drug-likeness properties of designed derivatives

Compounds	QED	NP score	Lipinski rule	Pfizer Rule	GSK Rule	Goldentriangle	Chelator rule
Native Ligand	0.202	-0.784	1	0	1	1	0
18beta-Glycyrrhetic_acid	0.464	3.183	0	1	1	0	0
Glabranin	0.826	2.083	0	1	1	0	0
Glabridin	0.832	2.496	0	1	1	0	0
Glycyrrhetic_acid	0.464	3.183	0	1	1	0	0
Hispaglabridin_A	0.676	2.748	0	1	1	0	0
Isoliquiritin	0.284	1.516	0	0	1	0	0
Licoflavone_A	0.702	1.482	0	1	0	0	0
Licoricesaponin_E2	0.149	2.591	1	0	1	1	0
Liquiritin	0.472	1.913	0	0	1	0	0

Table 5. Absorption parameter of selected compounds

Compounds	Caco-2 Permeability	MDCK Permeability	Pgp-inhibitor	Pgp- substrate	HIA	F20%	F30%	F50%
Native ligand	-4.59734	-4.60575	0.99977	0.004411	6.59E-05	4.34E-05	2.85E-05	0.045315
18beta- Glycyrrhetic_acid	-5.07173	-4.71832	4.70E-05	0.278493	2.26E-06	0.386072	0.003083	0.929365
Glabranin	-4.91284	-4.71302	0.983659	0.030698	0.002971	0.379595	0.991448	0.998854
Glabridin	-4.88944	-4.75905	0.108352	0.370878	2.38E-07	0.064906	0.43135	0.886096
Glycyrrhetic_acid	-5.24155	-4.96557	0.000275	0.241852	3.56E-05	0.608382	0.01079	0.97832
Hispaglabridin_A	-4.94488	-4.68143	0.179692	0.116669	2.86E-05	0.509255	0.364332	0.883458
Isoliquiritin	-6.06035	-5.20694	0.016158	0.00894	0.115027	0.556037	0.997171	0.98564
Licoflavone_A	-4.81593	-4.75118	0.019204	0.171483	0.041304	0.985385	0.995281	0.999041
Licoricesaponin_E2	-5.9772	-5.15208	3.98E-11	0.003001	0.000381	0.018112	0.00183	0.667391
Liquiritin	-6.41024	-5.03395	0.005	0.274764	0.916954	0.171971	0.987157	0.99685

Table 6. Distribution and metabolism parameter of selected molecules

Compounds	Distribution				Metabolism									
	PPB%	VD	BBB	Fu	CYP1A2		CYP2C19		CYP2C9		CYP2D6		CYP3A4	
					Inhibitor	Substrate	Inhibitor	Substrate	Inhibitor	Substrate	Inhibitor	Substrate	Inhibitor	Substrate
Native Ligand	97.55034	0.564534	0.000438	2.100958	0.012066	0.997732	0.957253	0.996786	0.999828	0.997216	0.000673	0.752398	0.95909	0.091143
18beta-Glycyrrhetic_acid	88.22602	-0.36194	0.095222	9.751969	6.15E-12	2.16E-07	1.57E-05	0.010603	1.05E-07	1.30E-10	4.44E-06	9.93E-10	0.001508	1
Glabranin	96.39595	0.573864	0.023049	3.440408	0.00145	0.003014	0.999999	0.065089	0.999982	0.002298	0.000762	0.001451	0.078033	0.000502
Glabridin	97.1374	0.400635	0.50553	2.781987	0.998149	0.420521	0.997333	0.508681	0.770886	0.98889	0.978272	0.961691	0.980612	0.130311
Glycyrrhetic_acid	89.96986	-0.35229	0.819939	8.323738	3.01E-13	0.007483	7.96E-05	0.950629	8.77E-06	0.001821	5.36E-08	1.83E-08	0.001047	0.993133
Hispaglabridin_A	95.78747	0.45298	0.370846	4.341311	0.957797	0.151772	0.999908	0.963096	0.992609	0.600773	0.897901	0.971435	0.988353	0.774112
Isoliquiritin	89.11369	-0.19345	0.001126	9.269788	0.003037	9.17E-05	0.001186	2.16E-08	0.0003	0.000404	0.013517	0.002469	0.000215	1.89E-08
Licoflavone_A	95.56743	0.1198	0.004408	3.550867	0.817633	7.35E-05	0.999999	0.981139	0.99871	0.235269	0.75054	0.994692	0.992746	0.003693
Licoricesaponin_E2	68.33821	-0.57305	0.000597	25.6714	5.51E-17	7.78E-09	2.47E-11	0.213161	8.04E-13	9.39E-08	8.73E-15	1.57E-12	7.09E-09	0.602853
Liquiritin	81.92177	-0.19785	0.000762	18.20338	4.88E-12	8.02E-05	5.23E-06	0.103948	0.001179	0.657339	1.57E-07	0.00093	0.005466	0.410778

Table 7. Excretion and toxicity parameters of selected compounds

Compounds	Excretion				Toxicity							
	CL-plasma	T _{1/2}	H-HT	DILI	Ames toxicity	Rat oral acute Toxicity	FDAMDD	Skin sensitization	Carcinogenicity	Eye corrosion	Eye irritation	Respiratory toxicity
Native Ligand	4.774751	2.114166	0.927706	0.951096	0.711508	0.794458	0.935316	0.341559	0.661456	1.09E-10	1.79E-05	0.99247
18beta-Glycyrrhetic_acid	3.045382	1.42584	0.670907	0.176423	0.1	0.315091	0.624686	0.987144	0.808966	0.174105	0.874065	0.755036
Glabranin	5.181621	1.165695	0.859223	0.656604	0.736199	0.894904	0.718772	0.980823	0.17797	0.001704	0.935188	0.958028
Glabridin	3.927336	1.730583	0.903946	0.121072	0.714568	0.668767	0.883752	0.851373	0.630302	0.014607	0.983303	0.60822
Glycyrrhetic_acid	1.283456	1.323882	0.74361	0.341793	0.176072	0.338635	0.709832	0.995882	0.873563	0.115171	0.884887	0.921872
Hispaglabridin_A	3.169188	1.626212	0.797819	0.716919	0.698063	0.896707	0.773396	0.946184	0.426181	0.000136	0.65653	0.997599
Isoliquiritin	2.550747	3.404769	0.631378	0.810675	0.839183	0.014223	0.090594	0.990097	0.144653	2.34E-05	0.675925	0.033735
Licoflavone_A	7.976144	1.358042	0.515609	0.789867	0.655987	0.710034	0.841819	0.804034	0.741974	0.012106	0.957297	0.840195
Licoricesaponin_E2	0.452726	3.823978	0.600007	0.966317	0.435107	0.086042	0.067366	0.999511	0.074394	2.01E-07	0.002233	0.009002
Liquiritin	2.437956	2.564347	0.692011	0.74268	0.731959	0.360047	0.330675	0.110096	0.522232	2.13E-06	0.338544	0.124667

Table 8. Environmental toxicity profile of designed molecules

Compounds	BCF	IGC50	LC50FM	LC50DM
Native Ligand	0.842411	3.712427	4.410223	4.979635
18beta-Glycyrrhetic_acid	0.77337	3.747967	4.631481	5.408158
Glabranin	1.935081	4.72405	5.688481	6.307322
Glabridin	1.812599	4.569415	5.37714	5.918796
Glycyrrhetic_acid	1.308899	4.0865	5.009328	5.703159
Hispaglabridin_A	2.249459	4.941959	6.016951	6.563765
Isoliquiritin	0.948053	3.712215	4.527526	5.07692
Licoflavone_A	1.649044	4.748696	5.353449	5.67277
Licoricesaponin_E2	0.44235	3.519689	4.466311	5.399467
Liquiritin	0.493687	3.148143	3.858228	4.959597

Physicochemical properties

Physicochemical descriptors are essential indicators of the oral bioavailability, permeability, and molecular interactions of a compound. The molecular weights (MW) of the selected compounds ranged between 322.12 and 820.39 Da. Compounds such as glabranin, glabridin, and licoflavone A possessed MW below 350 Da, consistent with Lipinski's rule of five, suggesting good membrane permeability and oral absorption. Conversely, larger molecules such as licorice saponin E2 (820.39 Da) may have reduced permeability due to their size; although, their glycosidic nature could contribute to biological activity.

The topological polar surface area (TPSA) ranged from 58.92 Å² (glabridin and hispaglabridin A) to 256.04 Å² (licoricesaponin E2). A TPSA below 140 Å² generally indicates favorable absorption and BBB penetration. Therefore, glabridin and hispaglabridin A may cross the BBB efficiently, whereas highly polar molecules such as isoliquiritin and licoricesaponin E2 are likely to remain restricted to the systemic circulation.

The logP and logS values further support these findings: glabranin (logP = 4.51) and hispaglabridin A (logP = 5.48) displayed higher lipophilicity, favoring membrane permeability but requiring metabolic caution, whereas liquiritin and isoliquiritin, with lower logP values (0.13–1.03), exhibited good aqueous solubility and enhanced oral absorption potential. Overall, glabridin, glabranin, and licoflavone A demonstrated optimal physicochemical balance for membrane permeability and solubility, whereas glycyrrhetic acid and 18β-glycyrrhetic acid provided moderate values supportive of bioavailability.

Drug-likeness properties

A drug-likeness assessment predicts how well a compound fits within known pharmacological frameworks. Quantitative Estimation of Drug-likeness (QED) values closer to 1 indicated a higher potential. Among the studied compounds, glabridin (QED = 0.832) and glabranin (QED = 0.826) showed superior scores, suggesting high compatibility with known drug-like chemical spaces. The moderate QED values for licoflavone A (0.702) and hispaglabridin A (0.676) further highlight their promising nature.

Natural product (NP) scores reflect the degree of structural novelty relative to the known natural scaffolds. 18 β -glycyrrhetic acid and glycyrrhetic acid had high NP scores (3.183), indicating distinct natural origins and complex scaffolds typical of triterpenoid compounds. Lipinski's rule compliance was observed for all compounds except the native ligand and licoricesaponin E2, both exceeded acceptable limits due to higher MW and hydrogen bond counts. All compounds satisfied the Pfizer and GSK filters, implying a low risk of mutagenicity and reactive toxicity.

Only a few compounds, such as licoflavone A, showed noncompliance with the Golden Triangle rule, which predicts an optimal pharmacokinetic and safety balance. Overall, glabridin, glabranin, and licoflavone A presented favorable drug-likeness parameters, supporting their potential as orally active agents.

Absorption properties

Effective absorption is crucial for its oral bioavailability. Caco-2 and MDCK cell permeability are predictive markers for intestinal and epithelial transport, respectively. Compounds such as glabridin and glabranin exhibited acceptable Caco-2 permeability values (-4.88 to -4.91) and strong fractional absorption (F50% > 0.88), suggesting efficient intestinal uptake. In contrast, isoliquiritin and licorice saponin E2 had low permeability values (< -6.0), implying limited passive diffusion due to high polarity.

The P-gp interaction parameters revealed key insights into their potential as P-gp inhibitors or substrates. Notably, glabranin (P-gp inhibitor = 0.983) and the native ligand (0.999) exhibited strong inhibitory potential, consistent with the study's aim to identify P-gp modulators. Conversely, glycyrrhetic acid and licoflavone A showed minimal inhibition probability (≤ 0.02), suggesting limited efflux interference. High Human Intestinal Absorption (HIA) values for licoflavone A (0.0413) and liquiritin (0.9169)

indicated favorable gastrointestinal absorption, which was further enhanced by excellent F30% and F50% scores.

Overall, glabranin and glabridin demonstrated the best absorption profiles, with strong P-gp inhibitory potential and high permeability, highlighting them as promising leads for overcoming MDR.

Distribution and metabolism

Distribution parameters, such as PPB and volume of distribution (VD), influence drug bioavailability and tissue diffusion. High PPB values (>95%) were noted for glabranin (96.39%) and glabridin (97.13%), suggesting extended plasma retention and longer half-life. Compounds with moderate PPB, such as licoflavone A (95.56%), may strike a balance between tissue distribution and circulation.

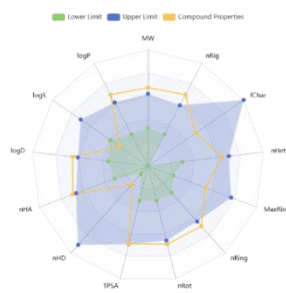
BBB permeability values indicated that glabridin (0.5055) and glycyrrhetic acid (0.8199) could potentially cross the BBB, which may be beneficial for neurological applications but requires further selectivity assessment. The free drug fraction (Fu) values also supported that glycyrrhetic acid and licoflavone A maintain sufficient unbound concentrations for systemic action.

CYP enzyme interactions revealed differential metabolic profiles. Glabridin and hispaglabridin A exhibited inhibitory effects against multiple CYP isoforms (notably CYP1A2 and CYP2C19), implying a possible modulation of hepatic metabolism. However, their strong inhibitory behavior toward CYP3A4 may necessitate caution in avoiding drug-drug interactions. Conversely, licoflavone A and glycyrrhizin acid showed balanced substrate affinity, ensuring a stable metabolism and predictable clearance.

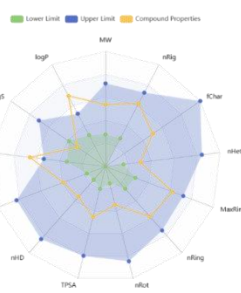
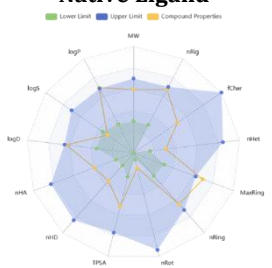
Excretion and toxicity

The excretion kinetics and toxicity parameters determine overall safety and the therapeutic window. The clearance (CL) and half-life ($T_{1/2}$)

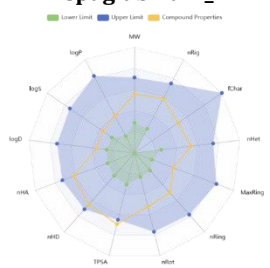
Table 9. ADMET radar of most potent compounds and native ligand



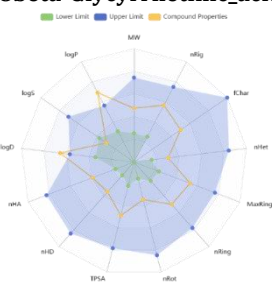
Native Ligand



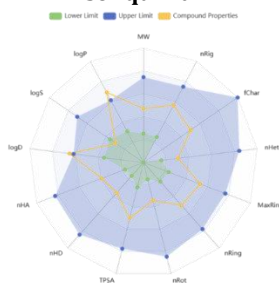
Hispaglabridin_A



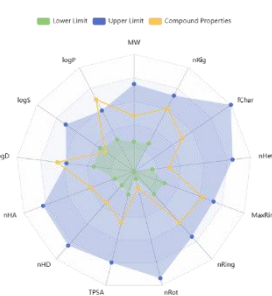
18beta-Glycyrrhetic_acid



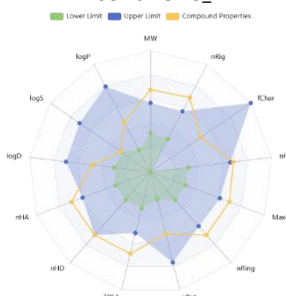
Isoliquiritin



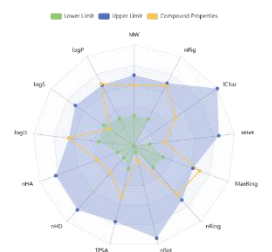
Glabranin



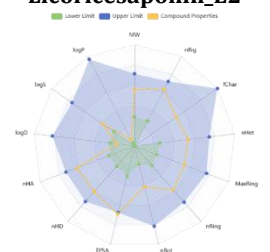
Licoflavone_A



Glabridin



Licoricesaponin_E2



Glycyrrhetic_acid

Liquiritin

values indicate the elimination rate and systemic retention. Licoflavone A demonstrated high clearance (7.97 mL/min/kg) with a moderate half-life (1.35 h), suggesting rapid and safe excretion. In contrast, licorice saponin E2 displayed the lowest clearance (0.45 mL/min/kg) and longest half-life (3.82 h), indicative of potential accumulation.

The toxicity profiles were generally favorable. Ames toxicity predictions showed non-mutagenic behavior for all compounds, and no significant carcinogenicity or skin sensitization was observed for glabridin, hispaglabridin A, and licoflavone A. The native ligand exhibited a higher toxicity risk (H-HT = 0.92, DILI = 0.95), emphasizing that the natural derivatives possess better safety margins. Rat oral acute toxicity and FDAMDD data also reflected acceptable tolerability, with most compounds within safe exposure ranges. Hispaglabridin A and glabranin demonstrate minimal organ toxicity, reinforcing their pharmacological safety.

Environmental toxicity

The environmental toxicity profile indicates that the candidate molecules pose minimal ecological hazards. Parameters such as the Bioconcentration Factor (BCF) and lethal concentration (LC50) values for fish and *Daphnia* were analyzed. All compounds exhibited BCF values below 3, indicating low bioaccumulation potential. Hispaglabridin A (IGC50 = 4.94, LC50FM = 6.01) and glabranin (LC50FM = 5.68) were relatively safe, demonstrating low aquatic toxicity. In contrast, liquiritin and licoricesaponin E2 showed slightly higher environmental toxicity due to their higher solubility and structural complexity but remained within acceptable ecological safety limits.

The ADMET radars for the most potent compounds with native ligands are listed in [Table 9](#). The integrated ADMET profile strongly supports glabridin, glabranin, and licoflavone A as

the most promising P-gp inhibitors among *Glycyrrhiza glabra* derivatives. These compounds exhibit ideal physicochemical attributes, optimal drug likeness, good intestinal absorption, balanced metabolism, and low toxicity risk. Their strong P-gp inhibitory potential suggests that they may effectively reverse MDR by enhancing intracellular drug accumulation in cancer cells. On the other hand, large glycosides, such as licorice saponin E2 and isoliquiritin, displayed limited permeability and high polarity, restricting their bioavailability. However, they may still contribute to synergistic effects when used in combination. In summary, computational ADMET analyses confirmed that glabridin, glabranin, and licoflavone A hold significant potential as lead molecules for further *in vitro* and *in vivo* validation as natural P-gp inhibitors derived from *Glycyrrhiza glabra*, potentially overcoming MDR and improving the therapeutic efficacy of co-administered drugs.

Conclusion

In conclusion, the current computational analysis effectively identified potent bioactive compounds from *Glycyrrhiza glabra* with significant potential to inhibit P-gp, a critical efflux transporter responsible for MDR in cancer and microbial infections. Twenty structurally diverse phytochemicals were selected from the literature and evaluated using molecular docking and *in silico* ADMET analyses to elucidate their binding affinities, pharmacokinetic profiles, and toxicity parameters. Among the tested compounds, 18 β -glycyrrhetic acid, glycyrrhetic acid, hispaglabridin A, glabridin, glabranin, and licoflavone A exhibited strong binding affinities (-8.3 to -9.7 kcal/mol) and stable interactions with key residues of P-gp, suggesting their ability to block substrate efflux and enhance intracellular drug accumulation. These findings are supported by multiple hydrogen bonds and hydrophobic interactions involving amino acids, such as

PHE343, GLN347, GLU875, and TYR310, which are crucial for ligand stabilization. ADMET profiling further revealed that compounds such as glabridin, glabranin, and licoflavone A possess favorable physicochemical characteristics, high intestinal permeability, acceptable metabolic stability, and minimal predicted toxicity, aligning well with the drug-likeness parameters. In contrast, large glycosylated saponins, although less permeable, display low toxicity and potential synergistic pharmacological roles. Collectively, this study demonstrated that selected G. glabra compounds, particularly glabridin, glabranin, and licoflavone A, represent promising lead molecules for the design of safe and effective natural P-gp inhibitors capable of mitigating MDR. Future studies will focus on MD simulations to assess the conformational stability and dynamic behavior of ligand–protein complexes over time, followed by *in vitro* P-gp inhibition assays, cytotoxicity evaluations in resistant cancer cell lines, and *in vivo* pharmacokinetic studies.

Disclosure Statement

No potential conflict of interest was reported by the authors.

ORCID

Karthickeyan Krishnan:

<https://orcid.org/0000-0002-1709-730X>

S. Gopi Krishnan:

<https://orcid.org/0009-0004-9425-1253>

Ch K V L S N Anjana Male:

<https://orcid.org/0000-0001-9032-8314>

Pericharla Venkata Narasimha Raju:

<https://orcid.org/0009-0003-2259-6693>

Phanindra Erukulla:

<https://orcid.org/0009-0001-2900-2881>

Kanaka Durga Hanumanthu:

<https://orcid.org/0009-0005-8402-410X>

Ashutosh Pathak:

<https://orcid.org/0009-0000-9158-9356>

Nampelly Karnakar:

<https://orcid.org/0000-0003-2471-6831>

References

- [1] Emran, T.B., Shahriar, A., Mahmud, A.R., Rahman, T., Abir, M.H., Siddiquee, M.F.-R., Ahmed, H., Rahman, N., Nainu, F., Wahyudin, E. **Multidrug resistance in cancer: Understanding molecular mechanisms, immunoprevention and therapeutic approaches.** *Frontiers in Oncology*, **2022**, 12, 891652.
- [2] Catalano, A., Iacopetta, D., Ceramella, J., Scumaci, D., Giuzio, F., Saturnino, C., Aquaro, S., Rosano, C., Sinicropi, M.S. **Multidrug resistance (MDR): A widespread phenomenon in pharmacological therapies.** *Molecules*, **2022**, 27(3), 616.
- [3] Bukowski, K., Kciuk, M., Kontek, R. **Mechanisms of multidrug resistance in cancer chemotherapy.** *International Journal of Molecular Sciences*, **2020**, 21(9), 3233.
- [4] Zahra, R., Furqan, M., Ullah, R., Mithani, A., Saleem, R.S.Z., Faisal, A. **A cell-based high-throughput screen identifies inhibitors that overcome P-glycoprotein (Pgp)-mediated multidrug resistance.** *Plos one*, **2020**, 15(6), e0233993.
- [5] Labbozzetta, M., Poma, P., Tutone, M., McCubrey, J.A., Sajeva, M., Notarbartolo, M. **Phytol and heptacosane are possible tools to overcome multidrug resistance in an *in vitro* model of acute myeloid leukemia.** *Pharmaceuticals*, **2022**, 15(3), 356.
- [6] Karthika, C., Sureshkumar, R., Zehravi, M., Akter, R., Ali, F., Ramproshad, S., Mondal, B., Tagde, P., Ahmed, Z., Khan, F.S. **Multidrug resistance of cancer cells and the vital role of P-glycoprotein.** *Life*, **2022**, 12(6), 897.
- [7] Zhang, H., Xu, H., Ashby Jr, C.R., Assaraf, Y.G., Chen, Z.S., Liu, H.M. **Chemical molecular-based approach to overcome multidrug resistance in cancer by targeting p-glycoprotein (P-gp).** *Medicinal Research Reviews*, **2021**, 41(1), 525–555.
- [8] Yu, J., Zhou, P., Asenso, J., Yang, X.-D., Wang, C., Wei, W. **Advances in plant-based inhibitors of P-glycoprotein.** *Journal of Enzyme Inhibition and Medicinal Chemistry*, **2016**, 31(6), 867–881.
- [9] Binkhathlan, Z., Lavasanifar, A. **P-glycoprotein inhibition as a therapeutic approach for overcoming multidrug resistance in cancer: Current status and future perspectives.** *Current Cancer Drug Targets*, **2013**, 13(3), 326–346.
- [10] Gandla, K., Islam, F., Zehravi, M., Karunakaran, A., Sharma, I., Haque, M.A., Kumar, S., Pratyush, K., Dhawale, S.A., Nainu, F. **Natural polymers as potential P-glycoprotein inhibitors: Pre-ADMET profile and computational analysis as a proof of**

- concept to fight multidrug resistance in cancer. *Heliyon*, **2023**, 9(9), e19454.
- [11] Zhang, J., Wu, X., Zhong, B., Liao, Q., Wang, X., Xie, Y., He, X. **Review on the diverse biological effects of glabridin**. *Drug Design, Development and Therapy*, **2023**, 17, 15–37.
- [12] Lee, G., Joung, J.-Y., Cho, J.-H., Son, C.-G., Lee, N. **Overcoming p-glycoprotein-mediated multidrug resistance in colorectal cancer: Potential reversal agents among herbal medicines**. *Evidence-Based Complementary and Alternative Medicine*, **2018**, 2018(1), 3412074.
- [13] Pastorino, G., Cornara, L., Soares, S., Rodrigues, F., Oliveira, M.B.P. **Liquorice (glycyrrhiza glabra): A phytochemical and pharmacological review**. *Phytotherapy Research*, **2018**, 32(12), 2323–2339.
- [14] Babich, O., Ivanova, S., Ulrikh, E., Popov, A., Larina, V., Frolov, A., Prosekov, A. **Study of the chemical composition and biologically active properties of glycyrrhiza glabra extracts**. *Life*, **2022**, 12(11), 1772.
- [15] Hasan, M.K., Ara, I., Mondal, M.S.A., Kabir, Y. **Phytochemistry, pharmacological activity, and potential health benefits of glycyrrhiza glabra**. *Heliyon*, **2021**, 7(6), e07240.
- [16] Caroline, M.L., Muthukumar, R.S., Priya, A.H.H., Nachiammai, N. **Anticancer effect of plectranthus amboinicus and glycyrrhiza glabra on oral cancer cell line: An invitro experimental study**. *Asian Pacific Journal of Cancer Prevention: APJCP*, **2023**, 24(3), 881–887.
- [17] Yu, X.-Y., Lin, S.-G., Zhou, Z.-W., Chen, X., Liang, J., Yu, X.-Q., Chowbay, B., Wen, J.-Y., Duan, W., Chan, E. **Role of p-glycoprotein in limiting the brain penetration of glabridin, an active isoflavan from the root of glycyrrhiza glabra**. *Pharmaceutical Research*, **2007**, 24(9), 1668–1690.
- [18] Tamboli, A., Tayade, S. **In-Depth investigation of berberine and tropane through computational screening as possible DPP-IV inhibitors for the treatment of T2DM**. *Journal of Pharmaceutical Sciences and Computational Chemistry*, **2025**, 1(1), 1–11.
- [19] Siddiqui, F., Makhloufi, R., Salah, M.E.-S., Mohamed, E., Hojjati, M. **Computational exploration of quinine and mefloquine as potential anti-malarial agents**. *Journal of Pharmaceutical Sciences and Computational Chemistry*, **2025**, 1(2), 106–115.
- [20] Ahmed, S., Tabassum, P., Falak, S., Ahmad, A., Shaikh, M. **Molecular docking and network pharmacology: Investigating vitis vinifera phytoconstituents as multi-target therapeutic agents against breast cancer**. *Journal of Pharmaceutical Sciences and Computational Chemistry*, **2025**, 1(2), 116–134.
- [21] Jadhav, S., Dighe, P. **Synthesis, In vitro evaluation, and molecular docking studies of novel pyrazoline derivatives as promising bioactive molecules**. *Journal of Pharmaceutical Sciences and Computational Chemistry*, **2025**, 1(3), 190–209.
- [22] Dang, L., Jin, Y., Yuan, Y., Shao, R., Wang, Y. **Licorice: Comprehensive review of its chemical composition, pharmacodynamics, and medicinal value**. *Acupuncture and Herbal Medicine*, **2024**, 4(1), 136–150.

HOW TO CITE THIS ARTICLE

K. Krishnan, S.G. Krishnan, C.K.V.L.S.N. Anjana Male, P.V. Narasimha Raju, P. Erukulla, A. Pathak, K. Durga Hanumanthu, N. Karnakar. **Molecular Docking and ADMET-Based Discovery of Glycyrrhiza glabra Bioactives as P-Glycoprotein Inhibitors for Combating Multidrug Resistance**. *Adv. J. Chem. A*, 2026, 9(5), 773-796.

DOI: [10.48309/ajca.2026.553659.1952](https://doi.org/10.48309/ajca.2026.553659.1952)

URL: https://www.ajchem-a.com/article_235650.html